Multiwavelength Raman Fiber Lasers Using Hi-Bi Photonic Crystal Fiber Loop Mirrors Combined With Random Cavities

A. M. R. Pinto, O. Frazão, *Member, IEEE, OSA*, J. L. Santos, *Member, IEEE, OSA*, and M. Lopez-Amo, *Senior Member, IEEE, Member, OSA*

***Abstract*—Different multiwavelength Raman fiber lasers based on a hybrid cavity setup are proposed. The lasing schemes are based in highly birefringent photonic crystal fiber loop mirrors combined with random cavities. The Hi-Bi PCF loop mirrors are characterized by an interferometric output; whereas the random mirrors are created by cooperative Rayleigh scattering due to Raman gain. This configuration allows suppression of Rayleigh associated noise growth, while taking advantage of it as an active part of the laser cavity, enhancing the achievable gain. The proposed fiber lasers present stable operation at room temperature although different output maxima and shapes depending on the fiber loop mirror/random mirror combination.**

***Index Terms*—Fiber optics, fiber laser, photonic crystal fibers, raman laser, Rayleigh scattering, random laser.**

I. Introduction

MULTIWAVELENGTH fiber lasers based in Raman amplification technology are of great importance in optical communication networks as a mean for span transmission achievement and capacity. Several approaches have been undertaken in order to improve Raman lasers technology and efficiency. A dual wavelength Raman laser, 200 km long, utilizing two different-wavelength fiber Bragg gratings with a "random" Rayleigh scattering mirror was experimentally demonstrated [1]. Some other approaches were made in order to obtain multiple tunable outputs, being by using an all-fiber asymmetric cavity composed by wideband chirped fiber Bragg grating and narrowband tunable fiber Bragg gratings to obtain robust Raman fiber laser [2]; or by using a novel free-spectral-range tunable comb filter based on a superimposed chirped fiber Bragg grating and a linear cavity formed by a bandwidth-tunable chirped fiber Bragg grating reflector for continuously tunable spacing multiwavelength lasing [3]. Other approaches were based in tunable and stable lasing through power distribution among different lasing channels by adjusting the pump powers [4], or by using a tunable dual section high birefringence fiber Sagnac loop filter [5]. Advances have also been made in order to obtain tunable lasing as well as to diminish the Rayleigh scattering associated noise typical of this kind of lasers, by taken advantage of it as a distributed mirror combined with a highly birefringent photonic crystal fiber loop mirror [6].

Multi-channel filters are of great importance in multiwavelength fiber lasers, since they introduce the interferometric signal allowing multiwavelength lasing. Numerous all-fiber filters have been introduced into fiber laser cavities in order to achieve multiwavelength lasing oscillations. Of all possible fiber filters, fiber loop mirrors (FLMs) stand out due to their low insertion loss, low cost, simple construction, polarization independence to input light and broadband spectral bandwidth [7], [8]. However, most fiber loop mirrors based in polarization maintaining fibers (PMFs) are affected by temperature changes, which results in slow drifts of the peak transmission power. To solve this problem, highly birefringent photonic crystal fibers (Hi-Bi PCFs) are being used in the place of PMF. Hi-Bi PCFs have high birefringence and ultralow thermal sensitivity. These properties make FLMs based in Hi-Bi PCFs extremely insensitive to temperature variations when compared to PMF based ones, leading to improved stability in multi-wavelength fiber lasers based in such filters [5], [9], [10]. Examples of this improved stability are multiwavelength fiber lasers based on the combination of single mode fiber (SMF) and Hi-Bi PCF [4], [11] or on a FLM of two-stage PMFs [12].

An intrinsic fundamental loss mechanism of an optical fiber is Rayleigh scattering (RS). When using Raman amplification besides losses due to RS there will also be losses due to double Rayleigh scattering (DRS). The long lengths of fiber used for Raman amplification make the Rayleigh scattering associated noise an issue. As the gain in Raman amplifiers increases so will RS and DRS, which eventually limits the achievable gain [13]. An interesting approach in order to diminish these losses is using this Rayleigh associated noise as an active part of the laser. It can be used as a distributed random mirror transforming what were losses in gain in the output signal [6], [14]. Lasers taking advantage of cooperative Rayleigh scattering as a self-feedback mechanism of Brillouin-Rayleigh scattering have been reported [15]–[17]. Schemes have been implemented by using four-wave mixing method through the use of reduced high nonlinear Bismuth-erbium doped fiber for

Manuscript received December 16, 2010; revised February 17, 2011; accepted March 19, 2011. Date of publication April 05, 2011; date of current version May 04, 2011. The authors are grateful to the Spanish Government project TEC2010-20224-C02-01 and European COST action TD 1001.

A. M. R. Pinto and M. López-Amo Sainz are with the Departamento de Ingeniería Eléctrica y Electrónica of Universidad Pública de Navarra, 31006 Pamplona, Spain (e-mail: anamargarida.rodriguez@unavarra.es).

O. Frazão and J. L. Santos are with Instituto de Engenharia de Sistemas e Computadores do Porto (INESC) and with Departamento de Física, Faculdade de Ciências of Universidade do Porto, 4169-007 Porto, Portugal.

Color versions of one or more of the figures in this paper are available online at http://ieeexplore.ieee.org.x

Digital Object Identifier 10.1109/JLT.2011.2134833

Brillouin-Raman multiwavelength lasing with comb generation [18], or high-reflectivity mirror in the linear cavity for distributed feedback [19], [20].

In this paper, different multiwavelength Raman fiber lasers based in the same structural setup are presented. The setup is based in highly birefringent photonic crystal fiber loop mirrors combined with random mirrors. The Hi-Bi PCF loop mirrors are characterized by an interferometric output spectrum dependent on the length of the fiber; while the random mirrors are created by cooperative Rayleigh scattering in the dispersion compensating fiber (DCF) as a result of the high Raman gain. The multiwavelength Raman fiber lasers will be presented while demonstrating that by changing the parameters of the DCF inducing the random mirror and the length of the Hi-Bi PCF in the FLM, different stable multiwavelength fiber lasers can be obtained.

II. Principle of Operation

The multiwavelength Raman fiber lasers proposed in this work are the result of a fiber structure that uses distributed random mirrors based in cooperative Rayleigh scattering. The fiber loop mirror acts as one discrete mirror having an interferometric signal output; the cooperative Rayleigh scattering is a direct consequence of the Raman gain in the DCF, which acts as a distributed random mirror. The principle of operation of both mirrors is exposed below.

A. Fiber Loop Mirror Based in a Hi-Bi PCF

The Hi-Bi PCF loop mirror is formed by an optical coupler spliced to a Hi-Bi PCF. The optical coupler splits the input signal equally into two counter propagating waves. These waves travel trough the optical path with different velocities, due to the birefringence of the fiber. After propagating around the loop, these waves will recombine at the coupler. The difference in the propagating wave's velocities will lead to a variable interference term in the output port.

The different propagation velocity of the waves in the FLM is due to the high birefringence (β) of the fiber. Birefringence is the physical parameter that relates the difference in refractive indexes of the propagation's axis: $\beta = n_y - n_x$. This difference in refractive indexes leads to a phase difference $(\Delta\phi)$ between the waves propagating in the Hi-Bi PCF

$$\Delta\varphi = \frac{2\pi\beta L}{\lambda} \tag{1}$$

where L is the length of the fiber and λ the wavelength of operation. The transmission spectrum of the Hi-Bi FLM is approximately a periodic function of the wavelength

$$T = \left[\sin\frac{\beta L}{\lambda}\cos(\theta_1 + \theta_2)\right]^2 \tag{2}$$

where θ_1 and θ_2 are the angles between light in the propagation axis at the end of the Hi-Bi PCF. The wavelength spacing $(\Delta\lambda)$ between two consecutive interference channels in the transmission spectrum is given by

$$\Delta\lambda = \frac{\lambda^2}{\beta L} \tag{3}$$

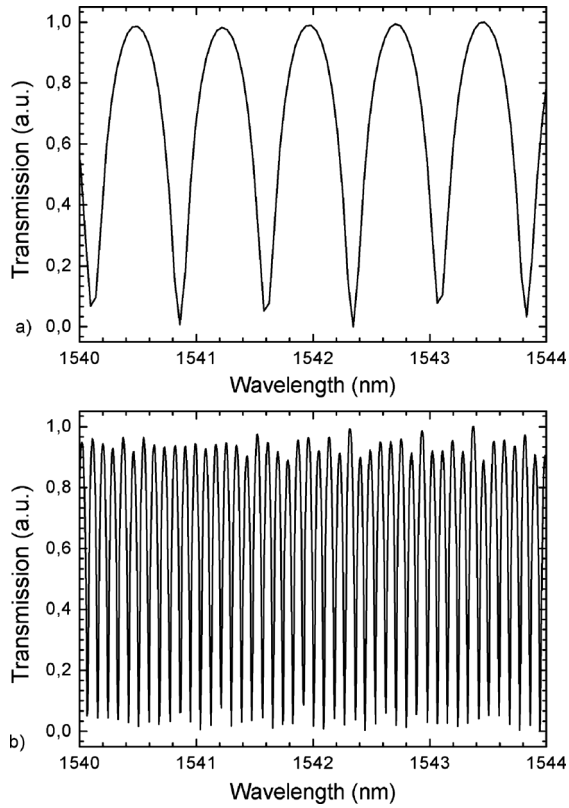

Fig. 1. Transmission spectrum of (a) FLM1 and (b) FLM2.

From (3), it can be seen that the wavelength spacing between two consecutive channels in a FLM is inversely proportional to the birefringence and length of the fiber. Its spectral characteristics are only dependent on these two parameters and, as so are independent of the polarization state of the input light [21].

The lasers proposed in this paper use the same Hi-Bi PCF (which means the same birefringence). Consequently from (3) one can expect that the wavelength spacing between two consecutive channels of the FLMs will only depend on the length of the Hi-Bi PCF used in the fiber loop mirror. This in turn means that the number of interference channels per nm as well as the spacing between them can be easily tailored by changing the length of the Hi-Bi PCF. Therefore, by simply altering the length of the Hi-Bi PCF one can insert more or less channels into the fiber loop mirror, which will be reflected on the final multiwavelength fiber laser. The multiwavelength fiber lasers are based in two fiber loop mirrors with different lengths of Hi-Bi PCF: FLM1 is composed by ∼3 m of Hi-Bi PCF and FLM2 has ∼30 m of Hi-Bi PCF. Fig. 1 presents the experimental transmission spectra for both FLMs, when illuminated by a broadband source. Since FLM1 has less length of Hi-Bi PCF its transmission spectrum presents more wavelength spacing than FLM2, and consequently fewer channels for the same wavelength range. FLM1 has ∼11 channels in a 10 nm range, with wavelength spacing between two consecutive channels of ∼0.9 nm; meanwhile FLM2 has ∼11 channels in 1nm range with a wavelength spacing of ∼0.09 nm.

B. Distributed Random Mirror

The random mirror is created by Rayleigh and double Rayleigh scattering in the DCF as an outcome of the Raman gain. In the moment that there is Raman gain in the DCF, RS is created. This first RS takes place in the counter-propagating direction of the signal and can undergo a second scattering event and co-propagate with the signal. This second RS is called double Rayleigh scattering. The DRS light will pass through the amplifier experiencing gain, and as a consequence appearing at the output as a noise source. Since these reflections will occur all along the fiber, the phase of the DRS light will fluctuate at the fiber output. As so, there will be time-delayed replicas of many signals guided in the propagating direction, leading to superpose signals and, consequently, noise. The Rayleigh associated noise when amplified by the Raman gain becomes the major source of power penalty in Raman amplified lightwave systems. As the gain in the Raman amplifier increases, so will the Rayleigh associated noise, which will eventually limit the achievable gain of the Raman amplifier [13].

Two different DCFs were used in this work: DCF1 with a dispersion of -343 ps/nm at 1545 nm, a compensation length of 20 km and an effective area of 21 μm^2, at 1550 nm; and DCF2 with a dispersion of -975 ps/nm at 1545 nm, a compensation length of 60 km and an effective area of 19 μm^2, at 1550 nm. The measured RS and DRS presented incoherent and instable spectra for both fibers. Rayleigh scattering presented higher power intensity (of the order of units of mW) than double Rayleigh scattering (of order of hundreds of μW), for both DCFs. The order of magnitude of these scatterings is understandable since RS is a direct consequence of the Raman scattering, while DRS is a consequence of the Rayleigh scattering. The DCF with less dispersion presented less powered spectra for both RS and DRS. Since RS and DRS depend on the Raman amplification, and this in turn depends on the amplification medium, it is to be expected that the fiber with less dispersion presents less powered distributed mirror.

III. Experimental Configuration

Four multiwavelength Raman fiber lasers are proposed based in the same structural set up, presented in Fig. 2. The set up consists in a high pump Raman laser at 1445 nm (maximum power of 3.3 W), an isolator (ISO), a fiber loop mirror, two wavelength division multiplexers (WDMs) and a dispersion compensating fiber. The signal output is read by an optical spectrum analyzer with a maximum resolution of 10 pm. The fiber loop mirror is formed by a 3 dB optical coupler (OC) with low insertion loss, a Hi-Bi PCF, and an optical polarization controller (PC) for optimized adjustment of the output spectrum. The Hi-Bi PCF (Thorlabs PM-1550-01) is a polarization maintaining photonic crystal fiber with optimal wavelength at 1550 nm, a beat length of 4 mm and an attenuation of 1.0 dB/Km (photograph in inset of Fig. 2). This Hi-Bi PCF presents two large holes around the core with a diameter of 4.5 μm and small holes in the cladding region with 2.2 μm of diameter. The pitch (spacing between the center of two adjacent holes) of this PCF is 4.4 μm, and the diameter of the holey region is 40 μm, whereas the outer diameter is 125 μm. The Hi-Bi PCF was spliced in both ends to a SMF using a conventional arc-electric fusion splicer machine [23], having the splices a maximum loss of 2 dB each.

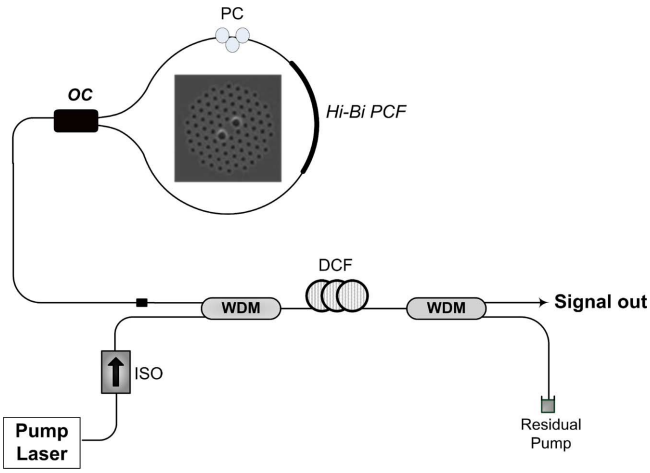

Fig. 2. Experimental set up for the multiwavelength Raman fiber lasers.

TABLE I
Lasers Detailed Constitution

	DCF1	*DCF2*
FLM1	**Laser 1**	**Laser 2**
FLM2	**Laser 3**	**Laser 4**

The differences between the four fiber lasers configuration consist on the length of the Hi-Bi PCF used in the FLM and/or in the value of dispersion of the DCF, as presented in Table I.

By using the scheme presented in Fig. 2, it is possible to take advantage of the RS associated noise as an active part of the laser, i.e., as a random mirror in the laser cavity, leading to the enhancement of the laser's performance. When there is Raman gain, the RS will be created in the DCF. Since RS contra-propagates with the signal it will travel to the FLM. During that path, a part of the RS will suffer again RS, thus creating DRS, and another part will reach the FLM. After traveling the FLM, the signal will travel throughout the DCF, experiencing Raman gain in the DCF, and thus RS and DRS again. These Rayleigh backscattered signals will induce incoherent multiple path interference, which are associated with the beating of multiple delayed replicas of the signal itself creating the distributed random mirror. The distributed mirror has a similar effect as two discrete reflectors with effective reflectance proportional to the ratios of total backscattered to incident power [24], [25].

IV. Results and Discussion

By varying the properties of the DCF inducing the random mirror and the Hi-Bi PCF constituting the FLM, four multiwavelength Raman fiber lasers with distinct characteristics were achieved. The multiwavelength fiber lasers based in FLM1 are presented in Fig. 3. For the same pump power, laser 1 and laser 2 present different wavelength range and number of channels. Laser 1 is characterized by stable and defined lasing channels in a wavelength range of 8 nm. The channel wavelength spacing is $\sim$0.875 nm. It presents a signal-to-noise ratio (SNR) of $\sim$17 dBm. In contrast, laser 2 presents an output spectrum with lasing channels in a wavelength range of 16 nm.

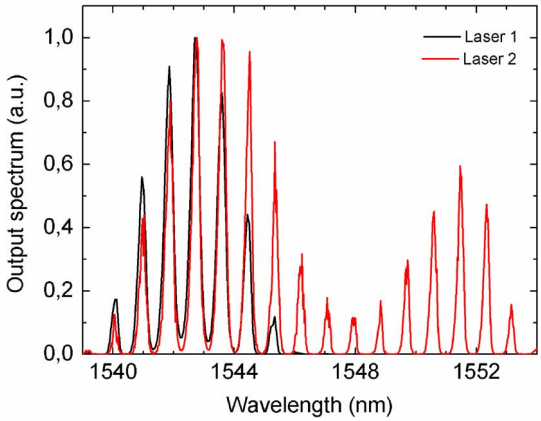

Fig. 3. Output spectra for laser 1 and laser 2.

The channel wavelength spacing is ∼0.85 nm and the SNR is ∼23 dBm. Despite of the fact that both lasers use the same FLM, laser 2 presents slightly smaller wavelength spacing between peaks. Even more, laser 2 presents higher SNR and wider wave length range and more lasing channels.

The number of lasing channels in the laser, and consequently the wavelength spacing between them, is limited by the Raman gain range and the length of the Hi-Bi PCF. The Raman gain range is imposed by the dopant, effective area and dispersion of the DCF. Since both DCFs present the same dopant, but different core effective areas and dispersion characteristics they have different Raman gain. The fiber with higher dispersion and lower effective area will present wider wavelength range and higher value of lasing channels, since the Raman gain is inversely proportional to effective area. But due to the fact that DCF2 has a wider lasing wavelength range, which leads to spread of the Raman gain throughout it, the final absolute output power of the laser is lower.

The multiwavelength fiber lasers based in FLM2 are presented in Figs. 4 and 5. Laser 3 output spectrum presented in Fig. 5 is characterized by ∼11 lasing channels per nm in a wavelength range of 10 nm. The channel wavelength spacing is ∼0.1 nm. Meanwhile, laser 4 presents an output spectrum also with ∼11 lasing channels per nm but in a wavelength range of 16 nm (see Fig. 5). The channel wavelength spacing is ∼0.09 nm. Similar to what occurred in lasers 1 and 2, lasers 3 and 4 present different wavelength ranges and slightly different wavelength spacing, due to the dispersion and effective area of the core in the DCFs used in each of the lasers. Laser 4, which uses the most dispersive and lower effective area DCF, presents a wider working wavelength range, but as a consequence the distributed mirror is spread over a wider range of wavelengths creating a less powerful laser, as it can be seen in Fig. 5. A common characteristic observed in lasers 3 and 4 that was also present in lasers 1 and 2 is the dislocation of the laser output spectrum for higher wavelengths due to the Raman gain. The higher the pump power is, more the spectrum shifts to higher wavelengths, transferring the power to higher wavelength channels. As a result, there is an increase of power for peaks situated at higher wavelengths. This characteristic behavior is a consequence of Raman amplification, given that the Raman gain is directly proportional to the pump power.

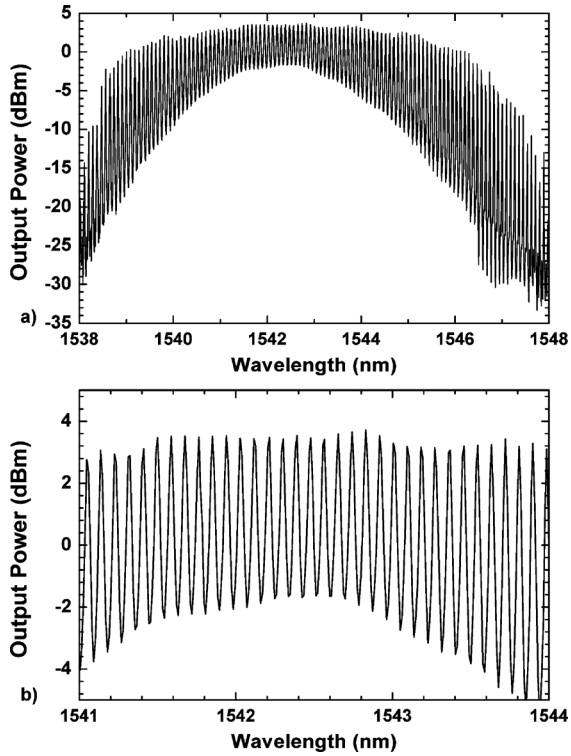

Fig. 4. Output power of laser 3 for (a) full span and (b) 3 nm span in the center of the spectrum; pump power 1.3 W.

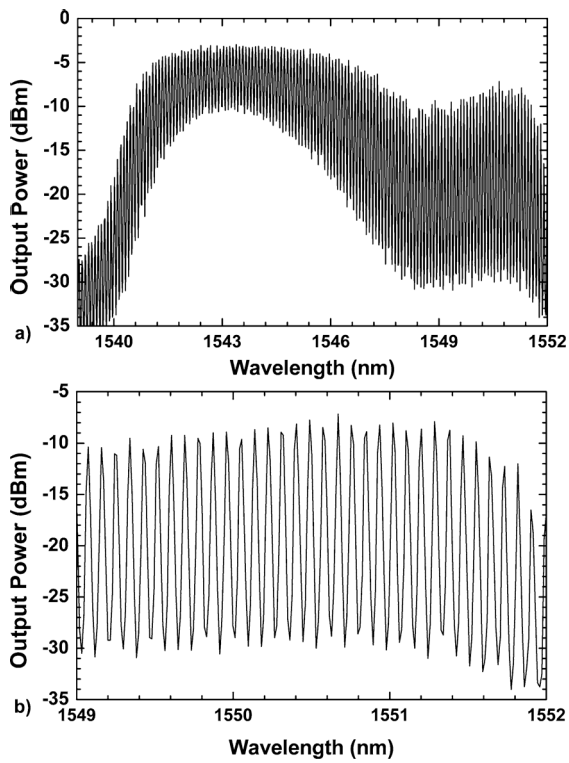

Fig. 5. Output power of laser 4 for (a) full span and (b) 3 nm span in the center of the spectrum; pump power 1.3 W.

In order to determine the stability of all four fiber lasers presented, the power fluctuations of the laser's lines were measured during one hour, in time intervals of 3 minutes. Fig. 6 presents

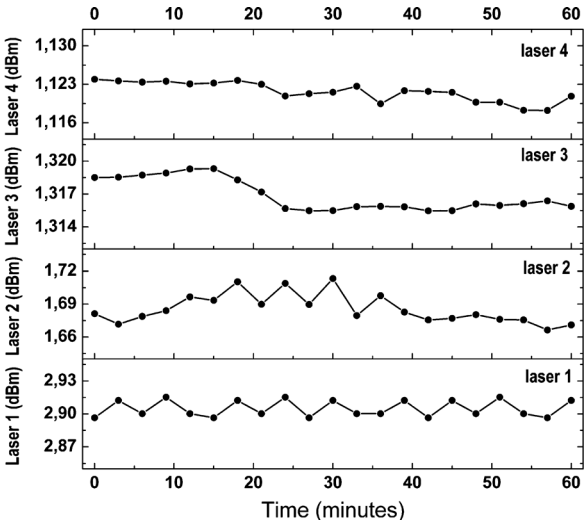

Fig. 6. Power fluctuations of an emission line of each of the four Raman fiber lasers.

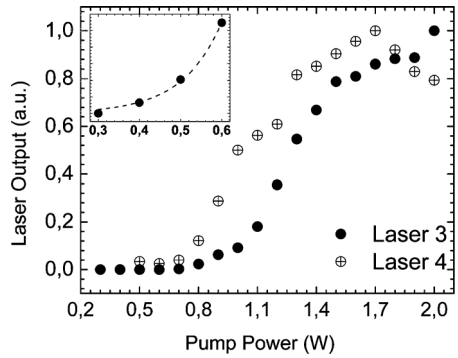

Fig. 7. Multiwavelength Raman fiber laser output power vs pump power, for laser 3 and laser 4. Inset: exponential growth of both lasers output for low pump powers, below the threshold pump power.

the optical power fluctuation for the central line of each of the proposed Raman fiber lasers. As it can be observed, the four lasers present little power fluctuations. In a time window of 60 minutes none of the emission lines exceeded 0.05 dBm of power fluctuations. High stability of these lasers was expected since they use FLMs, which have poor sensitivity to environmental noise, as well as temperature variations (due to the Hi-Bi PCF), and the Raman laser is known to be stable at room temperature. Specific applications such as long distance sensing illumination schemes and sensing interrogation [26] are adequate for this kind of lasers.

A. Other Considerations

Using the schematics presented in Fig. 2 and progressive pump power growth, it was observed that for pump powers lower than 1.3 W, the lasers present a different behavior than the presented above. For lower pump powers than 1.3 W, these lasers present two distinct regions of operation: a region characterized by a broadband output spectrum and another characterized by high instability. The broadband region starts when the first output spectrum of the laser can be obtained until reaching the instability region. The pump power for which this region starts depends on the FLM used in the laser. For lasers 1 and 2 (FLM1) the broadband region starts for a pump power of 0.2 W. While for lasers 3 and 4 (FLM2) this region only starts at 0.3 W pump power. Despite of the Hi-Bi PCF low insertion loss, for higher length this loss is more pronounced, leading to this difference. In this region, the output signal is characterized by a broadband spectrum presenting the interference due to the FLM of each laser. Lasers 1 and 3 present a lower output power value than lasers 2 and 4, owing to the DCF used to perform the laser. Lasers 2 and 4 were made with DCF2 which has more dispersion per km and lower effective area, leading to higher Raman gain. Notice that for such low powers the generation of DRS is so weak as to be negligible. As so, the backscattered Rayleigh scattering combined with the FLM and the Raman amplification will generate a broadband Fabry–Perot source in the gain wavelength range. The instability region starts at 0.7 W pump power for the lasers composed by DCF1 and 0.5 W for the lasers composed by DCF2. Is saying the pump power for which the instability starts depends on the DCF used in the laser. This instability region presents a corresponding optical spectrum with random spikes and dips characteristic of stochastic pulse generation. This high stability in the spectrum in the lower pump powers is followed by slowly development of the lasing spectrum, with lots of random spikes, until reaching the laser's threshold value, which is 1.3 W for all four lasers. This instability can be explained as the result of a destructive interference from all the time-delayed replicas of many multiple scattering signals guided in the propagating direction, which is the same as saying that there is a non cooperative rapport between the multiple Rayleigh scattering events. As the pump power increases, and the multiple scattering get stronger because there is higher Raman gain, these non cooperative rapport or destructive interference between the multiple scatterings will be less and less, until the pump power reaches its threshold value and a cooperative rapport or constructive interference between the replicas of the scattering events is obtained.

By measuring each fiber laser's output power for each pump power a characteristic response was founded. This response is similar for fiber lasers which use the same DCF. Laser 1 and laser 3 present almost identical responses, as do laser 2 and laser 4. Fig. 7 presents the normalized response of laser 3 and 4 as a function of the pump power. The lasers response is similar almost for all pump powers measured, excluding the higher pump powers. Both have an exponential response at lower pump powers (inset in Fig. 7), which is to be expected due to the Raman growth in the amplification medium. For higher pump powers a direct linear relationship between the laser output powers and the pump powers was obtained which was predictable since after passing the Raman threshold the Raman gain is proportional to the pump power. For pump powers reaching 1.7 W appears the main difference between both lasers regarding their dependence on the pump power. Laser 1 and laser 3, which structure contains DCF1, continue to have an almost directly linear relationship. However, when reaching and passing this pump power, laser 2 and laser 4 demonstrate an inverse relationship with the pump power. It seems like 1.7 W is the threshold value for saturation of DCF2's distribute mirror. This is saying, the cooperative rapport between RS

and DRS saturates at 1.7 W in DCF2, having afterwards a disparaging rapport. The value of the saturation power will be then dependent on the characteristics of the DCF. Since Raman gain depends on the gain medium (DCF), and Rayleigh scattering depends on the high Raman gain in the gain medium, one can conclude that the DCF characteristics will limit the Raman gain and distributed mirror, as well as its saturation pump power. Consequently, is should be expected that DCF1 presents the same behavior, although for higher pump powers than DCF2 since it was less dispersion.

V. Conclusion

Different multiwavelength Raman fiber lasers based in the combination of highly birefringent photonic crystal fiber loop mirrors combined with distributed random mirrors were presented and demonstrated. The Hi-Bi PCF loop mirrors had different interferometric output spectra dependent on the length of the fiber, which tailors the laser output spectrum shape. The distributed random mirrors presented different characteristic wavelength range and peak powers due to the different dispersion and effective area values of the DCFs used. The dispersion and effective area values of the DCF directly influence the Rayleigh scattering events created in the fiber, tailoring the characteristics of the distributed random mirror. Lasers containing a DCF with less dispersion and high effective area present higher maximum output peak power but lower wavelength range and less lasing channels; while lasers containing a DCF with more dispersion present a spread of the Raman gain throughout a wider wavelength range and more channels leading to a lower maximum output peak power. All lasers showed stable operation at room temperature, having maximum power fluctuations lower than 0.05 dBm over a one hour time window. For low pump powers the lasers act as broadband Fabry–Perot sources. The operation of each multiwavelength fiber laser has a characteristic dependence on the pump power, which is different for lasers that use different DCFs. From the proposed lasers it can be seen that lasers 1 and 2 present suitable characteristics to be used for sensing interrogation and multiplexation systems, whereas lasers 3 and 4 present proper qualities for dense wavelength division multiplexed systems. More different lasers can be obtained using this set up by only changing the length of the Hi-Bi PCF and/or the characteristics of the DCF. The set up proposed shows the ability for flexible tuning of the output spectrum shape and power. The laser's output characteristics can be easily tuned depending on the final intended application. Moreover, by simply adding more Raman pumps to the proposed set up, it is possible to equalize the output peak powers of the obtained fiber lasers by carefully adjusting the pump power of the additional Raman pumps.

One of the biggest advantages of using this configuration is the Rayleigh associated noise suppression, a known limitation of Raman lasers in communications systems. Using this configuration, the Rayleigh associated noise is suppressed while taking advantage of it as an active part in the laser cavity, the distributed random mirror. And, since higher Raman gain leads to higher Rayleigh associated noise, using this set up the consequence will be a stronger random mirror. This represents an important improvement in fiber optics communications, since there is an upgrade of the achievable gain in the amplifier. This ability to tailor the output spectrum and to suppress the Rayleigh associated noise makes lasers based on this set up suitable for lots of applications such as optical fiber sensors and optical sensing multiplexation systems, spectroscopy, optical instrument testing and measurements, microwave photonic systems and fiber optical communications systems.

References

[1] A. E. El-Taher, M. Alcon-Camas, S. A. Babin, P. Harper, J. D. Ania-Castanon, and S. K. Turitsyn, "Dual-wavelength, ultralong Raman laser with Rayleigh-scattering feedback," *Opt Lett.*, vol. 35, no. 7, pp. 1100–1102, Apr. 2010.

[2] Y. E. Im, S. Hann, H. Kim, D. H. Kim, and C. S. Park, "An all-fibre robust and tunable Raman fibre laser with reconfigurable asymmetric cavities," *Meas. Sci. Technol.*, vol. 20, no. 3, pp. 034022–034026, Mar. 2009.

[3] X. Y. Dong, P. Shum, N. Q. Ngo, and C. C. Chan, "Multiwavelength Raman fiber laser with a continuously-tunable spacing," *Opt. Exp.*, vol. 14, no. 8, pp. 3288–3293, Apr. 2006.

[4] D. R. Chen, S. Qin, L. F. Shen, H. Chi, and S. L. He, "An all-fiber multi-wavelength Raman laser based on a PCF Sagnac loop filter," *Microw Opt. Technol. Lett.*, vol. 48, no. 12, pp. 2416–2418, Dec. 2006.

[5] C. S. Kim, R. M. Sova, and J. U. Kang, "Tunable multi-wavelength all-fiber Raman source using fiber Sagnac loop filter," *Opt. Commun.*, vol. 218, no. 4–6, pp. 291–29, Apr. 2003.

[6] A. M. R. Pinto, O. Frazao, J. L. Santos, and M. Lopez-Amo, "Multiwavelength fiber laser based on a photonic crystal fiber loop mirror with cooperative Rayleigh scattering," *Appl. Phys. B.*, vol. 99, no. 3, pp. 391–395, Mar. 2010.

[7] D. B. Mortimore, "Fiber loop reflectors," *J. Lightw. Technol.*, vol. 6, no. 7, pp. 1217–1224, Jul. 1988.

[8] K. S. Lim, C. H. Pua, N. A. Awang, S. W. Harun, and H. Ahmad, "Fiber loop mirror filter with two-stage high birefringence fibers," *Progr. Electromag. Res. C*, vol. 9, pp. 101–108, 2009.

[9] D.-M. Liang, Y. Li, J.-H. Pei, Y. Jiang, Z.-H. Kang, and J.-Y. Gao, "Multi-wavelength fiber laser based on a highbirefringence fiber loop mirror," *Laser Phys. Lett.*, vol. 4, no. 1, pp. 57–60, Jan. 2007.

[10] D. H. Kim and J. U. Kang, "Sagnac loop interferometer based on polarization maintaining photonic crystal fiber with reduced temperature sensitivity," *Opt. Exp.*, vol. 12, no. 19, pp. 4490–4495, Sep. 2004.

[11] Z. Y. Liu, Y. G. Liu, J. B. Du, G. Y. Kai, and X. Y. Dong, "Tunable multiwavelength erbium-doped fiber laser with a polarization-maintaining photonic crystal fiber Sagnac loop filter," *Laser Phys. Lett.*, vol. 5, no. 6, pp. 446–448, Jun. 2008.

[12] J. Wang, K. Zheng, J. Peng, L. S. Liu, J. Li, and S. S. Jian, "Theory and experiment of a fiber loop mirror filter of two-stage polarization-maintaining fibers and polarization controllers for multiwavelength fiber ring laser," *Opt. Exp.*, vol. 17, no. 13, pp. 10573–10583, Jun. 2009.

[13] C. Headley and G. P. Agrawal, "Raman Amplification in Fiber Optical Communication Systems," in *Optics and Photonics*. London, U.K.: Elsevier Academic Press, 2005.

[14] A. K. Zamzuri, M. H. Al-Mansoori, N. M. Samsuri, and M. A. Mahdi, "Contribution of Rayleigh scattering on Brillouin comb line generation in Raman fiber laser," *Appl. Opt.*, vol. 49, no. 18, pp. 3506–3510, Jun. 2010.

[15] K. D. Park, B. Min, P. Kim, N. Park, J. H. Lee, and J. S. Chang, "Dynamics of cascaded Brillouin-Rayleigh scattering in a distributed fiber Raman amplifier," *Opt. Lett.*, vol. 27, no. 3, pp. 155–157, Feb. 2002.

[16] M. T. M. Giraldi, A. M. Rocha, B. Neto, C. Correia, M. E. V. Segatto, M. J. Pontes, A. P. L. Barbero, J. C. W. Costa, M. A. G. Martinez, O. Frazao, J. M. Baptista, H. M. Salgado, M. B. Marques, A. L. J. Teixeira, and P. S. Andre, "Rayleigh assisted Brillouin effects in distributed Raman amplifiers under saturated conditions at 40 Gb/S," *Microw. Opt. Technol. Lett.*, vol. 52, no. 6, pp. 1331–1335, Jun. 2010.

[17] B. Min, P. Kim, and N. Park, "Flat amplitude equal spacing 798-channel Rayleigh-assisted Brillouin/Raman multiwavelength comb generation in dispersion compensating fiber," *IEEE Photon. Technol. Lett.*, vol. 13, no. 12, pp. 1352–1354, Dec. 2001.

[18] S. Shahi, S. W. Harun, S. F. Norizan, M. R. A. Moghaddam, and H. Ahmad, "Brillouin-Raman multi-wavelength laser comb generation based on biEdf by using dual-wavelength in dispersion compensating fiber," *J. Nonlinear Opt. Phys.*, vol. 19, no. 1, pp. 123–130, Feb. 2010.

[19] A. K. Zamzuri, M. A. Mahdi, A. Ahmad, M. I. M. Ali, and M. H. Al-Mansoori, "Flat amplitude multiwavelength Brillouin-Raman comb fiber laser in Rayleigh-scattering-enhanced linear cavity," *Opt. Exp.*, vol. 15, no. 6, pp. 3000–3005, Mar. 2007.
[20] A. K. Zamzuri, M. I. M. Ali, A. Ahmad, R. Mohamad, and M. A. Mahdi, "Brillouin-Raman comb fiber laser with cooperative Rayleigh scattering in a linear cavity," *Opt. Lett.*, vol. 31, no. 7, pp. 918–920, Apr. 2006.
[21] O. Frazao, J. M. Baptista, and J. L. Santos, "Recent advances in high-birefringence fiber loop mirror sensors," *Sensors*, vol. 7, pp. 2970–2983, Nov. 2007.
[22] C. L. Zhao, X. F. Yang, C. Lu, W. Jin, and M. S. Demokan, "Temperature-insensitive interferometer using a highly birefringent photonic crystal fiber loop mirror," *IEEE Photon. Technol. Lett.*, vol. 16, no. 11, pp. 2535–2537, Nov. 2004.
[23] O. Frazao, J. P. Carvalho, and H. M. Salgado, "Low-loss splice in a microstructured fibre using a conventional fusion splicer," *Microw. Opt. Technol. Lett.*, vol. 46, no. 2, pp. 172–174, Jul. 2005.
[24] S. K. Turitsyn, S. A. Babin, A. E. El-Taher, P. Harper, D. V. Churkin, S. I. Kablukov, J. D. Ania-Castanon, V. Karalekas, and E. V. Podivilov, "Random distributed feedback fibre laser," *Nat. Photon.*, vol. 4, pp. 231–235, Feb. 2010.
[25] M. Z. I. J. L. Gimlett, N. K. Cheung, A. Righetti, F. Fontana, and G. Grass, "Observation of equivalent Rayleigh scattering mirrors in light wave systems with optical amplifiers," *IEEE Photonic. Technol. Lett.*, vol. 2, no. 3, pp. 211–213, Mar. 1990.
[26] M. Fernandez-Vallejo, S. Díaz, R. A. Perez-Herrera, D. Passaro, S. Selleri, M. A. Quintela, J. M. López, Higuera, and M. López-Amo, "Resilient long-distance sensor system using a multiwavelength Raman laser," *Meas. Sci. Technol.*, vol. 21, no. 9, pp. 094017–094022, Sep. 2010.

Ana Margarida Rodrigues Pinto was born in Porto, Portugal, in 1982. She received the physics degree from Universidade do Minho, Portugal, in 2006 and the M.S. degree in communications from Universidad Pública de Navarra, Navarra, Spain, in 2009, where she is currently working toward the Ph.D. degree.

From 2007 to 2008, she was with the Optoelectronics and Electronic Systems Unit of Inesc Porto, Portugal, working with a research grant. In the Ph.D. scope, she has done a research period in 2009 at the Optoelectronics and Electronic Systems Unit of Inesc Porto, Portugal, and in 2010 at the Brussels Photonics Team of the Vrije Universiteit Brussel, Belgium. Her present research interests include photonic crystal fibers, fiber optic sensing and optical communications.

Orlando Frazao graduated with a degree in physics engineering (optoelectronics and electronics) from the University of Aveiro, Portugal, and the Ph.D. degree in physics at the University of Porto, Portugal, in 2009.

From 1997 to 1998, he was with the Institute of Telecommunications, Aveiro. Presently, he is a Researcher at Optoelectronics and Electronic Systems Unit, INESC Porto. He has published about 250 papers, mainly in international journals and conference proceedings, and his present research interests included optical fiber sensors and optical communications.

Dr. Frazâo is a member of the Optical Society of America (OSA) and SPIE.

Jose Luis Santos graduated in 1983 with a Degree in applied physics (optics and electronics) from the University of Porto, Portugal, where he received the Ph.D. degree in physics in 1993 for research on fiber optic sensing.

He is an Associate Professor in the Physics Department, University of Porto. His main research interest is optical fiber sensing.

Prof. Santos is a member of the Optical Society of America (OSA), the International Society for Optical Engineers (SPIE) and European COST TD 1001 action.

Manuel Lopez-Amo (M'91–SM'98) was born in Madrid, Spain, in 1960. He received the telecommunications engineering degree and Ph.D. degrees from the Universidad Politécnica de Madrid, Spain in 1985 and 1989, respectively.

From 1985 to 1996, he belonged to the Photonic Technology Department of the Universidad Politécnica de Madrid, where in 1990 he became an Associate Professor. He has been a visiting researcher at INTEC of the University of Ghent, Belgium and at British Telecom Research Laboratories, Ipswich, U.K. In 1996, he moved to the Public University of Navarra, Pamplona, Spain, where he became a Full Professor in the Electrical and Electronic Engineering department and he is currently the head of the optical communications group of this department. He has been Chairman of the Optoelectronic Committee of Spain. He has been leader of more than 20 research projects and he has coauthored more than 150 works in international refereed journals and conferences related with fiber-optic networks, optical amplifiers, fiber-optic sensors, and integrated optics.

Prof. Lopez-Amo is a member of the technical committees of the International Conference on fiber optic sensors (OFS), the European Workshop on optical fiber sensors (EWOFS), and European COST TD 1001 action, among others. He is senior member of the OSA.